J. Fluid Mech. (2000), *vol.* 420, *pp.* 201–223. Printed in the United Kingdom

Thermal generation of Alfvén waves in oscillatory magnetoconvection

By PAUL H. ROBERTS AND KEKE ZHANG†

Institute of Geophysics and Planetary Physics, University of California, Los Angeles, CA 90095-1567, USA

(Received 7 December 1998 and in revised form 26 April 2000)

Marginal convection in the form of Alfvén waves in an electrically conducting Bénard layer in the presence of a vertical magnetic field is investigated analytically using the Boussinesq model for the fluid. Small amplitude solutions are studied using the linearized magnetoconvection equations. These solutions are represented by double expansions in terms of two small parameters: a dimensionless viscosity and a dimensionless magnetic diffusivity. The leading-order problem corresponds to undamped Alfvén waves propagating between the boundaries of the fluid; buoyancy forces appear at higher order and can maintain the Alfvén waves against viscous and ohmic damping. The structure of the Alfvén waves is strongly dependent, even at leading order, on the physical nature of the walls. Four different types of boundary conditions are considered here: (A) illustrative, i.e. mathematically simple conditions, (B) solid, perfectly conducting walls, (C) vacuum external to the layer, and (D) solid, perfectly insulating walls. It is shown how in each case Alfvén waves are excited by a small, but sufficiently strong, thermal buoyancy but that, because of boundary layers, the solutions for the four sets of boundary conditions are very different.

1. Introduction; basic equations

One of the classical problems of magnetohydrodynamics (MHD) is that of convection in a plane horizontal layer of an electrically conducting Boussinesq fluid across which a vertical magnetic field is applied. The linear stability problem was first studied by Thompson (1951) and later by Chandrasekhar (1952), who summarized the theory in Chapter 3 of his well-known book (Chandrasekhar 1961, which we shall refer to herein as C61).

Since C61 was published, the theory has been developed in a number of ways, especially through the inclusion of compressibility, finite-amplitude effects and even transition to turbulence. See for example Hurlburt *et al.* (1989) and Nordlund, Galsgaard & Stein (1993). Very often the main motivation has been to understand better magnetoconvection in the Sun and lower main sequence stars, and usually the boundary conditions that are mathematically the simplest have been employed. These are sometimes called the 'standard boundary conditions', e.g. see Blanchflower, Rucklidge & Weiss (1998). We shall refer to them as 'illustrative boundary conditions'. When these are used, the eigenfunctions of the linear stability problem are simple trigonometric functions and the Rayleigh number at which convection is marginally possible is a simple algebraic expression in terms of the wavenumber and the parameters

† Permanent address: School of Mathematical Sciences, University of Exeter, Exeter, EX4 4QJ, UK.

defining the fluid; there are no boundary layers no matter how strong the applied vertical magnetic field B_0 is.

This situation must be regarded as exceptional. For example, it is well known that Hartmann layers arise on no-slip boundaries when B_0 is large. These boundary layers exert a long-range effect on solutions far from the boundaries. Not surprisingly therefore quantities such as the marginal Rayleigh number may be drastically different from their values for the illustrative boundary conditions. This is established below, along with analogous results for other boundary conditions.

A second objective of this paper is to study magnetoconvection in parameter ranges in which the role of Alfvén waves is exhibited in the clearest possible way. We shall therefore concentrate on situations in which these waves are only lightly damped; more precisely, we shall suppose that

$$\eta_v \equiv v/Vd \ll 1, \tag{1.1}$$

$$\eta_\lambda \equiv \lambda/Vd \ll 1, \tag{1.2}$$

where v is the kinematic viscosity of the fluid, λ is its magnetic diffusivity, d is the depth of the layer, $V = B_0/\sqrt{\mu\rho}$ is the Alfvén speed, μ is the magnetic permeability and ρ is the fluid density; SI units are used. As a result of (1.1) and (1.2), oscillatory convection takes the form of Alfvén waves propagating between the boundaries, lightly damped viscously and ohmically, but refreshed by the buoyancy provided by heating the layer at its bottom boundary $\left(z = -\frac{1}{2}d\right)$ and cooling it at its top boundary $\left(z = \frac{1}{2}d\right)$.

It is appropriate here to introduce other dimensionless numbers. The third diffusivity that arises is κ, the thermal diffusivity, which is given dimensionlessly by

$$\eta_\kappa \equiv \frac{\kappa}{Vd}, \tag{1.3}$$

and which is assumed to be $O(1)$. The three η-parameters are closely related to the usual Prandtl numbers:

$$P_r = \frac{v}{\kappa} = \frac{\eta_v}{\eta_\kappa}, \quad P_m = \frac{v}{\lambda} = \frac{\eta_v}{\eta_\lambda}, \quad P_q = \frac{\lambda}{\kappa} = \frac{\eta_\lambda}{\eta_\kappa}. \tag{1.4}$$

We shall not employ the Hartmann number

$$M = \frac{Vd}{\sqrt{v\lambda}} = \frac{1}{\sqrt{\eta_v\eta_\lambda}} = \frac{1}{\eta_\lambda P_m^{1/2}}, \tag{1.5}$$

or the Chandrasekhar number $Q = M^2$. As a measure of the temperature gradient, β, across the layer we shall use

$$R = \frac{g\alpha\beta d^2}{V^2}, \tag{1.6}$$

where α is the coefficient of volume expansion and g is the acceleration due to gravity. The Rayleigh number more usually employed is $g\alpha\beta d^4/v\kappa = R/\eta_v\eta_\kappa$; see C61, (105) of Chap. 2.

To realize our second objective, it is convenient to depart slightly from the traditional non-dimensionalization of the governing equations; see C61, Chap. 3, (118). We use

$$t \to (d/V)t, \quad \boldsymbol{x} \to \boldsymbol{x}d, \quad \boldsymbol{u} \to V\boldsymbol{u}, \quad \boldsymbol{B} \to B_0\boldsymbol{B}, \quad T \to T\beta d, \tag{1.7}$$

where $\boldsymbol{u}$ is fluid velocity, $\boldsymbol{B}$ is magnetic field and T is temperature; the unperturbed

state is $\boldsymbol{u} = 0$, $\boldsymbol{B} = \mathbf{1}_z$ and $\nabla T = -\mathbf{1}_z$ where $\mathbf{1}_z$ is the unit upward vector. The perturbations in $\boldsymbol{B}$ and T away from this state will be written as $\boldsymbol{b}$ and θ. The unit of energy dissipation per unit time (and per unit horizontal area of the layer) is ρV^3. In C61, Chap. 3, the linear equations governing θ, $\boldsymbol{u}$, $\boldsymbol{b}$ and the pressure perturbation were reduced to scalar equations for θ, the vertical velocity w (our u_z) and h_z (our b_z). We shall use instead θ, ϕ and h where

$$\boldsymbol{u} = \nabla \times \nabla \times (\phi \mathbf{1}_z), \quad \boldsymbol{b} = \nabla \times \nabla \times (h \mathbf{1}_z), \tag{1.8}$$

so that w and h_z are our $-\nabla_H^2 \phi$ and $-\nabla_H^2 h$, where ∇_H is the horizontal divergence. (Perturbations in vertical vorticity and vertical electric current are excluded automatically in (1.8). It is easily shown that, even if these are initially present, they will disappear as $t \to \infty$, since they have no energy source to maintain them against viscous and ohmic losses.)

The basic equations are now

$$\left(\frac{\partial}{\partial t} - \eta_v \nabla^2\right) \nabla^2 \phi = \nabla^2 \frac{\partial h}{\partial z} - R\theta, \tag{1.9}$$

$$\left(\frac{\partial}{\partial t} - \eta_\lambda \nabla^2\right) h = \frac{\partial \phi}{\partial z}, \tag{1.10}$$

$$\left(\frac{\partial}{\partial t} - \eta_\kappa \nabla^2\right) \theta = -\nabla_H^2 \phi. \tag{1.11}$$

On seeking normal mode solutions of the form

$$\phi(x, y, z, t) \to \phi(z) \exp\left[\mathrm{i}(k_x x + k_y y - \omega t)\right], \text{ etc.}, \tag{1.12}$$

in the usual way, we obtain

$$\left(\mathrm{D}^2 - a^2 - \frac{\mathrm{i}\omega}{\eta_v}\right)(\mathrm{D}^2 - a^2)\phi = -\frac{1}{\eta_v}(\mathrm{D}^2 - a^2)\mathrm{D}h + \frac{R}{\eta_v}\theta, \tag{1.13}$$

$$\left(\mathrm{D}^2 - a^2 - \frac{\mathrm{i}\omega}{\eta_\lambda}\right) h = -\frac{1}{\eta_\lambda}\mathrm{D}\phi, \tag{1.14}$$

$$\left(\mathrm{D}^2 - a^2 - \frac{\mathrm{i}\omega}{\eta_\kappa}\right) \theta = -\frac{a^2}{\eta_\kappa}\phi, \tag{1.15}$$

where $a = (k_x^2 + k_y^2)^{1/2}$ is the total horizontal wavenumber and $\mathrm{D} = \mathrm{d}/\mathrm{d}z$ cf. C61, Chap. 3, (119)–(121). Without loss of generality we may assume that $\mathrm{Re}(\omega) \geqslant 0$.

2. Boundary conditions

Equations (1.13)–(1.15) define an eighth-order system of ordinary differential equations. When its solutions are subjected to eight boundary conditions it defines an eigenvalue problem for ω. A marginal state is defined as the smallest value of R for given a for which $\mathrm{Im}(\omega) = 0$. If $\mathrm{Re}(\omega)$ is also zero, the marginal state is steady; otherwise it is oscillatory. The critical state is the marginal state with the smallest R as a function of a. The eight boundary conditions, four at $z = -\frac{1}{2}$ and four at $z = \frac{1}{2}$, depend on the physical nature of the walls and what lies beyond them.

It is usual to suppose that the boundaries are perfect thermal conductors on which

T can adjust instantaneously to the temperatures at which they are held. It then follows that

$$\theta = 0 \quad \text{at } z = \pm\tfrac{1}{2}. \tag{2.1}$$

Consider next conditions placed on $\boldsymbol{b}$ by electromagnetic theory. If the exterior of the fluid is free space or is a solid dielectric, there are no currents flowing in it, and therefore $\nabla^2 h = 0$ so that, in $z > \frac{1}{2}$ (say),

$$h(z) = A\, \mathrm{e}^{-az}, \tag{2.2}$$

for some constant A. Since $\boldsymbol{b}$ is continuous it follows that

$$\mathrm{D}h \pm ah = 0 \quad \text{at } z = \pm\tfrac{1}{2}, \tag{2.3}$$

where we have also included the corresponding condition on $z = -\frac{1}{2}$. A popular alternative to (2.3) supposes that the walls are perfect electrical conductors. Strictly speaking this idealization can be used only for oscillatory convection, and then only if the electromagnetic penetration depth, $\delta_w = (\eta_\lambda^w/\omega)^{1/2}$, is small compared with unity, where η_λ^w refers to the walls (Gibson 1966). If the upper boundary is a solid, $\boldsymbol{b}$ is essentially zero for $z - \frac{1}{2} > \delta_w$, so that (since b_z must be continuous)

$$h = 0 \quad \text{at } z = \pm\tfrac{1}{2}. \tag{2.4}$$

In general $\mathrm{D}h$ and therefore $\boldsymbol{b}$ are not continuous; there are surface currents on the walls.

Finally consider $\boldsymbol{u}$. If the boundaries are fixed solids, $\boldsymbol{u}$ is zero on them, and by (1.8)

$$\phi = \mathrm{D}\phi = 0 \quad \text{at } z = \pm\tfrac{1}{2}. \tag{2.5}$$

A popular alternative to (2.5) is to assume that there is no exchange of momentum between fluids and walls, the so-called 'stress-free' conditions. Suppose the exterior $z > \frac{1}{2}$ of the layer is free space. The convective motions infinitesimally distort the boundary so that it is no longer flat. Usually the frequency of surface gravity waves on the free boundary greatly exceeds the reciprocal of the characteristic convective time scales such as $1/\omega$. In this case, the condition that the normal component of stress should be continuous reduces to $\phi = 0$, i.e. the distortions of the boundary are negligible. The total tangential component of stress on the boundary is the sum of the tangential components of the viscous and magnetic stresses, but since $\boldsymbol{b}$ is continuous the magnetic stresses are automatically continuous. Free space provides no viscous stress, so we simply have $\mathrm{D}^2\phi = 0$. In short

$$\phi = \mathrm{D}^2\phi = 0 \quad \text{at } z = \pm\tfrac{1}{2}. \tag{2.6}$$

There are a number of different situations of interest.

Case A: The illustrative boundary conditions:

$$\phi = \theta = 0, \quad \mathrm{D}^2\phi = \mathrm{D}h = 0 \quad \text{at } z = \pm\tfrac{1}{2}. \tag{2.7a–d}$$

Case B: The boundaries are stationary perfect conductors:

$$\phi = \theta = 0, \quad \mathrm{D}\phi = h = 0 \quad \text{at } z = \pm\tfrac{1}{2}. \tag{2.8a–d}$$

Case C: Beyond the boundaries is free space:

$$\phi = \theta = 0, \quad \mathrm{D}^2\phi = \mathrm{D}h \pm ah = 0 \quad \text{at } z = \pm\tfrac{1}{2}. \tag{2.9a–d}$$

Case D: The boundaries are stationary insulators:

$$\phi = \theta = 0, \quad \mathrm{D}\phi = \mathrm{D}h \pm ah = 0 \quad \text{at } z = \pm\tfrac{1}{2}. \tag{2.10a–d}$$

Conditions A, (2.7), are the simplest and therefore the most popular boundary conditions to apply. Condition (2.7*d*) is the special case (when the toroidal field vanishes) of the more general demands

$$B_x = B_y = \mathrm{D}B_z = 0 \quad \text{at } z = \pm\tfrac{1}{2}, \tag{2.11a–c}$$

where strictly (2.11*c*) is superfluous, since it follows from (2.11*a*), (2.11*b*) and $\boldsymbol{\nabla}\cdot\boldsymbol{B} = 0$. Conditions (2.11*a*)–(2.11*c*) and corresponding statements for spherical geometry are commonplace in studies of magnetoconvection and fluid dynamos, especially in astrophysical and solar contexts; see for example Gilman & Miller (1981), Hurlburt *et al.* (1989), Wang, Sheeley & Nash (1991) and Kageyama *et al.* (1995). Conditions C are applicable also when a light, perfectly insulating fluid fills the exterior of the layer. Conditions A–D by no means exhaust all possibilities. It has been argued (e.g. Parker 1974) that Alfvénic radiation from a sunspot umbra is significant, and to model this it is necessary to make the upper boundary transparent to Alfvén waves. This has been done by linking convection in the unstable layer to motions in an overlying neutrally stable region; see Musman (1967) and Savage (1969).

When the convection is steady, the magnetic conditions (2.7*d*), (2.8*d*), (2.9*d*) and (2.10*d*) have little significance. This is because, when $\omega = 0$, the system (1.13)–(1.15) factorizes into a sixth-order problem, consisting of (1.15) together with

$$(\mathrm{D}^2 - a^2)^2\phi = \frac{1}{\eta_v\eta_\lambda}\mathrm{D}^2\phi + \frac{R}{\eta_v}\theta, \tag{2.12}$$

and the second-order problem (1.14). Once (1.15) and (2.12) have been solved, which is done without reference to the conditions on h, the eigenvalue R is known and one need not return to (1.14) to find h. We shall focus here on oscillatory convection, for which the eighth-order problem does not factorize and for which a boundary condition on h is required.

In what follows we shall ignore situations in which one of A, B, C or D applies on $z = \frac{1}{2}$ and a different one on $z = -\frac{1}{2}$. We shall analyse Cases A, B, C and D in §§ 3, 4, 5 and 6, respectively. The paper concludes (§ 7) with a few remarks and a summary.

3. Case A: illustrative boundary conditions

Conditions (2.7*a*)–(2.7*d*) are commonly used in studies of magnetoconvection in the Sun, where many physical processes operate that complicate the modelling considerably. One difficulty arises from the transition from the main convection zone to the solar atmosphere. This is often evaded by the simple expedient of introducing an upper ('cut-off') boundary at some convenient level in the upper convection zone; see e.g. Gilman & Miller (1981) and Glatzmaier (1984). The question of what boundary conditions should best be applied on that boundary is not easily answered, but the general perception is that the illustrative conditions can be adopted because other boundary conditions should (*a*) give qualitatively identical results, and (*b*) introduce quantitative differences that are insignificant in comparison with the consequences of other idealizations inherent in the model. Examples of the complications of modelling solar magnetoconvection include the influence of the upper cut-off and the concomitant alteration in layer depth (see § 3 of Nordlund *et al.* 1994), the effects of radiative transfer (Steiner *et al.* 1994), variations in opacity in the convection zone, assumptions made about the applied magnetic field (if not dynamo created), and so on.

As noted in § 2, condition (2.7*d*) implies (2.11*a*)–(2.11*c*), i.e. that the magnetic field is vertical on the wall. There is some observational support for this (see e.g. conclusion 10 of Howard & Labonte 1981), and it is sometimes suggested that magnetic buoyancy is responsible. This has not, to our knowledge, been established theoretically, and to attempt a demonstration here would require us to change our model fundamentally by introducing compressibility and by analysing how the region above the convecting layer could be represented by a boundary condition on the upper boundary of the layer. The resulting complications would blur our principal message that boundary layers can create substantial changes to the asymptotic laws that hold in their absence. While the Sun provides one of the main applications of magnetoconvection theory, its study lies far beyond the scope of this paper, which is concerned with filling a substantial gap in general magnetoconvection theory that has existed for the last four decades.

Chandrasekhar derived (2.3) and (2.4) in C61, Chap. 3, § 42(b), but condition (2.7*d*) did not arise. This is not surprising. If we disregard (2.11*a*)–(2.11*c*) because of their uncertain theoretical status in solar magnetoconvection (a topic not addressed in C61, Chap. 3), there is no context in which (2.7*d*) is even approximately true. Nevertheless, (2.7*d*) was basic to the analysis in C61, Chap. 3, § 46. The reason for this appears to have been mathematical expediency. Conditions (2.7*a*)–(2.7*d*) lead to simple eigenfunctions such as

$$\phi \propto \cos \pi z, \quad h \propto \sin \pi z, \quad \theta \propto \cos \pi z, \tag{3.1}$$

and to simple algebraic expressions for ω^2 and R; there are no boundary layers. In the limits (1.1) and (1.2) of small viscous and ohmic dissipation, it is readily shown that

$$\omega \sim \pi \left[1 - \frac{\eta_v + \eta_\lambda}{2\eta_\kappa}\right], \tag{3.2}$$

$$R \sim \eta_\kappa(\eta_v + \eta_\lambda)\frac{\pi^2 + a^2}{a^2}\left[(\pi^2 + a^2)^2 + \frac{\pi^2}{\eta_\kappa^2}\right], \tag{3.3}$$

which are consistent with C61, Chap. 3, (230) and (231).

If $\eta_\kappa \ll 1$ (where as usual η_v/η_κ and η_λ/η_κ are nevertheless small), (3.2) and (3.3) agree with (241) of C61, Chap. 3 for the preferred mode

$$a_c \sim \frac{\pi^{2/3}}{2^{1/6}\eta_\kappa^{1/3}}, \quad R_c \sim \pi^2 \frac{(\eta_v + \eta_\lambda)}{\eta_\kappa}. \tag{3.4}$$

When $\eta_\kappa \gg 1$, (3.3) gives

$$a_c \sim \frac{\pi}{\sqrt{2}}, \quad R_c \sim \frac{27\pi^4}{4}\eta_\kappa(\eta_v + \eta_\lambda). \tag{3.5}$$

If in addition $P_m \gg 1$, the critical wavenumber and the critical value of Chandrasekhar's Rayleigh number $R_c/\eta_v\eta_\kappa$ are identical to those of the non-magnetic Bénard problem for stress-free boundaries (C61, § 15a), but that solution is steady whereas the solution here oscillates with frequency (3.2). Even the present simple model highlights the dangers of doing the obvious, namely arguing that, because $P_r \ll 1$ and $P_q \ll 1$ in the solar convection zone, ν and λ can be set to zero at the outset; see for example equations (17)–(19) of Musman (1967), equations (11)–(13) of Savage (1969), and equations (1)–(3) of Parker (1974). Obviously the result of setting $\nu = \lambda = 0$ is to obtain an R_c that is independent of ν and λ, although it is clear from

η_κ	a_c	$R_c/\eta_\kappa(\eta_v+\eta_\lambda)$
0.01	8.61	1.198×10^5
0.10	3.70	2.654×10^3
1.00	2.27	686.7
5.00	2.22	658.7

TABLE 1. Some results for Case A.

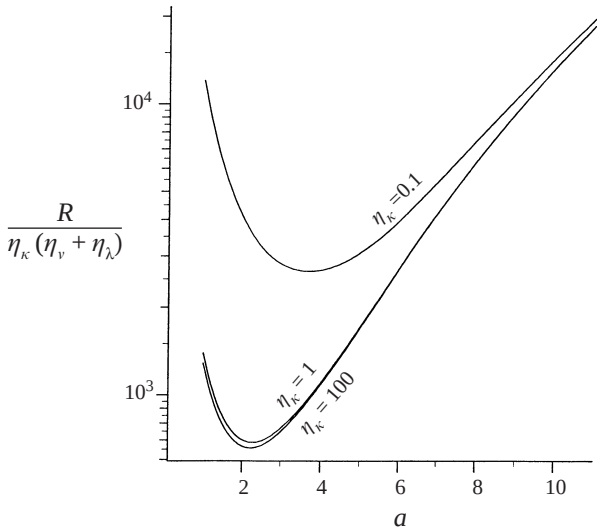

FIGURE 1. The neutral curves for thermal Alfvén waves in Case A when $P_m=1$ for various values of η_κ. The critical Rayleigh number R_c is scaled.

(3.3)–(3.5) that this conclusion is questionable. We shall find that the same difficulty arises in Cases B–D also.

Some results for Case A at intermediate values of η_κ are given in table 1.

Figure 1 shows the R_c given by (3.3) as a function a for three values of η_κ.

4. Case B: solid, perfectly conducting walls

4.1. *Undamped Alfvén waves*

In order that convective motions be dominantly Alfvén waves, it is necessary that both diffusion parameters, η_v and η_λ, be sufficiently small: $\eta_v \ll 1$ and $\eta_\lambda \ll 1$. This suggests that it is appropriate to express the mainstream solution (as we shall call the solution outside the boundary layers) through double expansions in η_v and η_λ of the form

$$R=\sum_{n=0}\sum_{k=0}\eta_v^n\eta_\lambda^k\,R_{nk},\quad \omega=\sum_{n=0}\sum_{k=0}\eta_v^n\eta_\lambda^k\,\omega_{nk},\quad \phi=\sum_{n=0}\sum_{k=0}\eta_v^n\eta_\lambda^k\,\phi_{nk},\qquad (4.1a\text{–}c)$$

and similarly for h and θ. Because of the effects of the Hartmann layers on the walls, however, these expansions are not tenable beyond $n=1$ and $k=1$; indeed, (4.1) itself is already incorrect in Case D (see § 6). It should be stressed that, even though both η_v and η_λ tend to zero, the solutions depend on the relative rate with which they do

so, i.e. on the magnetic Prandtl number P_m. How many and which terms are required in (4.1) depends on the magnitude of P_m.

Substituting expansions (4.1) into equations (1.13)–(1.15), we find that, to leading order for the mainstream,

$$\mathrm{i}\omega_{00}(\mathrm{D}^2 - a^2)\phi_{00} = (\mathrm{D}^2 - a^2)\mathrm{D}h_{00} - R_{00}\theta_{00}, \tag{4.2a}$$

$$\mathrm{i}\omega_{00}h_{00} = \mathrm{D}\phi_{00}, \tag{4.2b}$$

$$\left[\eta_\kappa(\mathrm{D}^2 - a^2) - \mathrm{i}\omega_{00}\right]\theta_{00} = -a^2\phi_{00}. \tag{4.2c}$$

That the differential order of equations (4.2*a–c*) is less than that of (1.13)–(1.15) is not surprising, as we expect thin boundary layers at the walls in which ϕ and h adjust to the boundary conditions and in which $\mathrm{D}\phi$ and $\mathrm{D}h$ are large, reflecting the high vorticity and high electric current densities existing in these layers. What is more surprising is that, despite omitting D^2 terms from both (1.13) and (1.14), the differential order of (4.2*a–c*) is still six, i.e. only two less than that of (1.13)–(1.15). This means that ϕ_{00}, h_{00} and θ_{00} must obey three of the four conditions derived in § 2 at each boundary, but which three? The answer is obvious only here where by (4.2*b*) h_{00} and $\mathrm{D}\phi_{00}$ vanish together at the walls:

$$\phi_{00} = \theta_{00} = h_{00} = 0 \quad \text{at } z = \pm\tfrac{1}{2}. \tag{4.3a–c}$$

At the leading order, described by (4.2)–(4.3), there are no diffusive effects, and no buoyancy source is required to maintain the disturbance. It follows that $R_{00} = 0$. Consequently, (4.2*c*) decouples from (4.2*a*, *b*), leaving behind a fourth-order equation that governs undamped Alfvén waves:

$$(\mathrm{D}^2 + \omega_{00}^2)(\mathrm{D}^2 - a^2)\phi_{00} = 0. \tag{4.4}$$

There are two distinct families of solutions: even modes with symmetry $\phi_{00}(z) = \phi_{00}(-z)$ and odd modes with symmetry $\phi_{00}(z) = -\phi_{00}(-z)$. For the even modes, we have, from (4.4) and condition (2.8*a*), (for $\omega_{00} \neq \pm\mathrm{i}a$)

$$\phi_{00} = \frac{\cos\omega_{00}z}{\cos\frac{1}{2}\omega_{00}} - \frac{\cosh az}{\cosh\frac{1}{2}a}, \tag{4.5a}$$

$$h_{00} = \mathrm{i}\left(\frac{\sin\omega_{00}z}{\cos\frac{1}{2}\omega_{00}} + \frac{a\sinh az}{\omega_{00}\cosh\frac{1}{2}a}\right). \tag{4.5b}$$

The boundary condition (4.3*c*) gives the dispersion relationship for ω_{00}:

$$\omega_{00}\tan\tfrac{1}{2}\omega_{00} + a\tanh\tfrac{1}{2}a = 0, \tag{4.6}$$

which has real roots (and the spurious roots $\omega_{00} = \pm\mathrm{i}a$ ruled out above). The modes given by (4.5*a*) have an even number of zeros in $-\frac{1}{2} < z < \frac{1}{2}$. To the ϕ_{00} having no zeros in the interval there corresponds the smallest ω_{00}, which is shown as a function of a in figure 2; for this mode

$$\omega_{00} \to \pi \quad \text{as } a \to \infty, \qquad \omega_{00} \to 2\pi \quad \text{as } a \to 0, \tag{4.7a,b}$$

facts that will be useful in § 6.2. It is found below that the marginal state (the most unstable convection mode) always corresponds to the smallest ω_{00}. We shall later focus on this and also ignore modes from the odd family below.

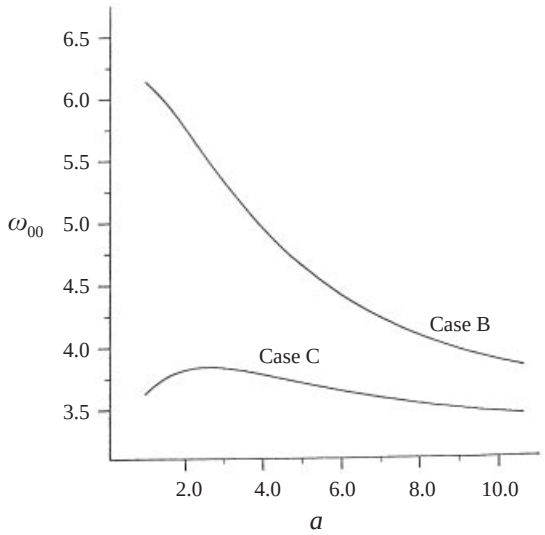

FIGURE 2. Solution of the dispersion relations for undamped Alfvén waves in Cases B and C. The solution having the smallest frequency ω_{00} is shown as a function of a. This is also the mode associated with the most easily excited mode of magnetoconvection, i.e. the mode having the smallest Rayleigh number. Modes B and C are also relevant to cases considered in § 6.3 and § 6.4, respectively.

For the second family having an odd number of zeros in $-\frac{1}{2} < z < \frac{1}{2}$,

$$\phi_{00} = \frac{\sin \omega_{00} z}{\sin \frac{1}{2}\omega_{00}} - \frac{\sinh az}{\sinh \frac{1}{2}a}, \tag{4.8a}$$

$$h_{00} = -\mathrm{i}\left(\frac{\cos \omega_{00} z}{\sin \frac{1}{2}\omega_{00}} - \frac{a \cosh az}{\omega_{00} \sinh \frac{1}{2}a}\right), \tag{4.8b}$$

and

$$\omega_{00} \cot \tfrac{1}{2}\omega_{00} - a \coth \tfrac{1}{2}a = 0. \tag{4.9}$$

The structure of the solutions is given by (4.5) and (4.8). The first terms on their right-hand sides arise from the vanishing of the first operator $(\mathrm{D}^2 + \omega_{00}^2)$ in (4.4). From the scaling (1.7) it is clear that these represent Alfvén waves of frequency ω_{00}. These waves are not however the transverse, xy-independent Alfvén waves of classic MHD. They depend on x and y and, to satisfy (4.3a, c), they must be accompanied by gradients in the perturbed pressure, p, which, because the fluid is incompressible, is transmitted with infinite acoustic speed and therefore obeys $\nabla^2 p = 0$. This gives rise to the second terms on the right-hand sides of (4.5) and (4.8), which are associated with the vanishing of the second operator $(\mathrm{D}^2 - a^2)$ in (4.4). Such non-transverse waves are sometimes termed 'slow waves' or even 'slow magnetosonic waves'.

There is a second dissimilarity between (4.5) and (4.8) and the classic Alfvén wave. After substituting (4.5a) or (4.8a) into (4.2c) and solving subject to (4.3b), we determine θ_{00}, and this is non-zero. This shows that the perturbed field and flow are associated with a perturbed temperature that arises from the advection and diffusion of the mean temperature profile. To highlight this difference from the classic Alfvén wave, we shall call the disturbances in our convecting layer 'thermal Alfvén waves'. They are analogous to the thermal inertial waves we studied previously for the rotating

Bénard layer (Zhang & Roberts 1997). They are not similar to the thermally driven Alfvén waves studied by Musman 1967, Savage (1969) and Parker (1974), which are thermally damped even at leading order; see equations (2), (3) and (27) of Musman, equations (1) and (17) of Savage, and equations (20), (35) and (37) of Parker.

4.2. *Thermal Alfvén waves*

At leading order, then, the stability issue does not arise and $R_{00} = 0$. Undamped Alfvén waves propagate across $-\frac{1}{2} < z < \frac{1}{2}$, carrying a passive, thermally created, density stratification with them. To solve the stability problem, it is necessary to take the mainstream solution beyond (4.5), by including more terms in the expansion (4.1). Viscous and ohmic dissipation of the Alfvén waves arises in the higher-order problem, and can only be offset by the thermal buoyancy provided by a sufficiently large Rayleigh number R.

The case $P_m \gg 1$. It is the size of the magnetic Prandtl number that determines which additional terms are required for the stability problem. In this case, only one additional term ($n = 1$, $k = 0$) is needed from our expansions (4.1). The corresponding governing equations at this order are

$$(\mathrm{D}^2 - a^2)\,(\mathrm{i}\omega_{00}\phi_{10} - \mathrm{D}h_{10}) = -R_{10}\theta_{00} + (\mathrm{D}^2 - a^2)^2\phi_{00} - \mathrm{i}\omega_{10}(\mathrm{D}^2 - a^2)\phi_{00}, \quad (4.10a)$$

$$\mathrm{i}\omega_{00}h_{10} - \mathrm{D}\phi_{10} = -\mathrm{i}\omega_{10}h_{00}. \quad (4.10b)$$

When the Hartmann layers on the walls are analysed, it is readily seen that, to leading order in the boundary layer expansions, the vertical flow and the vertical magnetic field are independent of z, so that by conditions (2.8a) and (2.8d)

$$\phi_{10} = h_{10} = 0 \quad \text{at } z = \tfrac{1}{2}. \quad (4.11a, b)$$

(For a general discussion about Hartmann boundary layers, see, for example, Roberts 1967.) In (4.11), $z = \frac{1}{2}$ refers to the common edge of the boundary layer and the mainstream, i.e. the conditions apply to the mainstream solution. (The corresponding boundary conditions on $z = -\frac{1}{2}$ are redundant because of the symmetry of the solution with respect to $z = 0$.) At the order to which we are now working, the Hartmann layers play no further role. It may however be worth recalling that, when (as here) $P_m \gg 1$, the Hartmann layer resembles a viscous shear layer in which the vorticity is large; when integrated across the layer, the vorticity becomes a surface vorticity which is associated with a jump in the horizontal components of $\boldsymbol{u}$ across the layer. In contrast, the integrated volume currents in the layer are negligible at leading order, and the surface current to which these give rise when integrated across the layer is also negligible; the jump in $\boldsymbol{b}$ can therefore be disregarded. The situation is reversed when (as below) $P_m \ll 1$. The Hartmann layer then resembles a magnetic diffusion layer across which the horizontal components of $\boldsymbol{b}$ suffer discontinuities while those of $\boldsymbol{u}$ does not.

The temperature θ_{00} is no longer passive and in (4.10a) drives the Alfvén waves against the viscously dominated dissipation. From (4.2c) together with (4.3b) and (4.5a), we can determine θ_{00} uniquely:

$$\theta_{00} = \frac{a^2}{\eta_\kappa\Omega + \mathrm{i}\omega_{00}}\left[\frac{\cos\omega_{00}z}{\cos\frac{1}{2}\omega_{00}} - \frac{\mathrm{i}\eta_\kappa\Omega}{\omega_{00}}\frac{\cosh(X + \mathrm{i}Y)z}{\cosh\frac{1}{2}(X + \mathrm{i}Y)}\right] + \frac{\mathrm{i}a^2\cosh az}{\omega_{00}\cosh\frac{1}{2}a}, \quad (4.12)$$

where

$$\Omega = \omega_{00}^2 + a^2, \quad X = \frac{a}{\sqrt{2}}\left(1 + \sqrt{1 + \frac{\omega_{00}^2}{a^4\eta_\kappa^2}}\right)^{1/2}, \quad Y = \frac{\omega_{00}}{\sqrt{2}a\eta_\kappa}\left(1 + \sqrt{1 + \frac{\omega_{00}^2}{a^4\eta_\kappa^2}}\right)^{-1/2}.$$

The inhomogeneous equations (4.10) in general have no solution unless the associated solvability condition, which determines the marginal state of magnetoconvection, is satisfied. We have used two different ways to obtain the solvability condition. The first one was to solve (4.10) explicitly. Eliminating two undetermined integral constants by demanding that the two boundary conditions (4.11) are satisfied yields the solvability condition. The second method is to multiply (4.10*a*) by ϕ_{00}^*, the complex conjugate of ϕ_{00}, multiply (4.10*b*) by h_{00}^*, sum the results, and then integrate across the layer. Although the same answer is obtained, we found that the first approach is the simpler.

The form of the leading-order solutions, ϕ_{00} and h_{00}, on the right-hand side of equations (4.10*a*, *b*) suggests that the general solution for ϕ_{10} can be written as

$$\phi_{10} = A\frac{\cosh az}{\cosh \frac{1}{2}a} + B\frac{\cos \omega_0 z}{\cos \frac{1}{2}\omega_0} - C_1\frac{z\sinh az}{\cosh \frac{1}{2}a} - C_2\frac{z\sin \omega_0 z}{\cos \frac{1}{2}\omega_0} - C_3\frac{\cosh(X + \mathrm{i}Y)z}{\cosh \frac{1}{2}(X + \mathrm{i}Y)}. \quad (4.13)$$

While A and B are constants of integration to be determined by the boundary conditions, coefficients C_1, C_2 and C_3 are determined by direct substitution as

$$C_1 = \frac{R_{10}a}{2\Omega}, \quad C_2 = \frac{\mathrm{i}}{2}\left(\frac{R_{10}a^2}{\Omega(\eta_\kappa\Omega + \mathrm{i}\omega_{00})} - \Omega - 2\mathrm{i}\omega_{10}\right), \quad C_3 = \frac{\mathrm{i}R_{10}a^2\eta_\kappa^3\Omega}{\omega_0(\eta_\kappa\Omega + \mathrm{i}\omega_{00})^2}.$$

With ϕ_{10} given by (4.13), h_{10} can be obtained directly from equation (4.10*b*). The satisfaction of the two boundary conditions (4.11) leads to a complex solvability condition from which the real part and imaginary part yields two equations. One determines R_{10} at the onset of instability in the form of a thermal Alfvén wave, and the other makes a small correction to the Alfvén wave frequency:

$$R_{10} = \frac{\Omega}{\eta_\kappa a^2}\left(\frac{\Omega_+\left[\omega_{00}^2 + aT(aT-2)\right]}{\omega_{00}^2 + aT(aT-2) + 4\Omega_+\eta_\kappa^2\Omega G_r}\right), \quad (4.14)$$

$$\omega_{10} = -\frac{\omega_{00}R_{10}}{2\Omega}\left(\frac{a^2 + aT(2-aT)}{\omega_{00}^2 - aT(2-aT)} + \frac{a^2}{\Omega_+} - \frac{4a^2\eta_\kappa^3\Omega^2 G_i}{\omega_{00}\left[\omega_{00}^2 - aT(2-aT)\right]}\right), \quad (4.15)$$

where

$$G_r = ([\Omega_- X + 2\omega_{00}\eta_\kappa\Omega Y]\sinh X + [2\omega_0\eta_\kappa\Omega X - \Omega_- Y]\sin Y - aT\Omega_- C)/\Omega_+^2 C,$$

$$G_i = ([\Omega_- Y - 2\omega_{00}\eta_\kappa\Omega X]\sinh X + [2\omega_0\eta_\kappa\Omega Y + \Omega_- X]\sin Y + 2\Omega\omega_{00}aT\eta_\kappa C)/\Omega_+^2 C,$$

$$\Omega_\pm = \Omega^2\eta_\kappa^2 \pm \omega_{00}^2, \quad T = \tanh \tfrac{1}{2}a, \quad C = \cosh X + \cos Y.$$

It may be noticed that only one dissipation parameter, η_κ, appears in equation (4.14). Evidently, if the leading-order solution is to be an undamped Alfvén wave, η_κ must be sufficiently large compared with η_ν, i.e. $P_r \ll 1$. It is also clear that the minimization of the Rayleigh number R_{10} over the wavenumber a using expressions (4.14) and (4.6) has to be carried out numerically. Our evaluations of $R_{10}(a, \eta_\kappa)$

η_κ	a_c	R_c/P_r	ω_{00}
0.01	11.9	18.1	3.75
0.10	5.6	65.4	4.50
1.00	3.3	1.86×10^3	5.22
5.00	3.1	4.37×10^4	5.30

TABLE 2. Typical examples for Case B, $P_m \gg 1$.

η_κ	a_c	R_c/P_r	ω_{00}
0.01	12.9	24.38	3.70
0.10	5.6	101.68	4.50
1.00	3.0	2.562×10^3	5.43
5.00	2.8	5.903×10^4	5.43

TABLE 3. Typical examples for Case B, $P_m \ll 1$.

strongly suggest that, for any given value of η_κ, there always exists a most unstable mode that is characterized by a minimum Rayleigh number, $R_c = (R_{10}P_r)_{\min}$ and a corresponding critical wavenumber a_c. Although we expect that $a_c \sim \eta_\kappa^{-1/2}$ when $\eta_v \ll \eta_\kappa \ll 1$, the expression (4.14) cannot be significantly simplified in this case. When $\eta_\kappa \gg 1$, we expect an optimal balance between the dissipation of the thermal Alfvén waves and the driving buoyancy at an $a_c = O(1)$ wavenumber. In this case, (4.14) can be substantially simplified. The leading-order asymptotic expression for R_{10} may be written as

$$R_{10} \sim \frac{\eta_\kappa \Omega^3 \left[\omega_{00}^2 + aT(aT-2)\right]}{a^2 \left[\omega_{00}^2 + aT(aT-2)\right] + \omega_{00}^2(\Omega F_1 + 4aF_2)} \quad \text{for } \eta_\kappa \to \infty, \tag{4.16}$$

where

$$F_1 = \frac{1}{4}\left[-aT^3 + T^2 + \left(a + \frac{2}{a}\right)T - 1\right], \quad F_2 = \frac{a}{2}(1-T^2) + T.$$

Also (4.15) shows that

$$\omega_{10} \to 0 \quad \text{as } \eta_\kappa \to \infty. \tag{4.17}$$

Table 2 gives several typical examples calculated from (4.6) and (4.14). This table shows that $a_c = 3.3$ and $R_c/\eta_\lambda\eta_v = 1860$ for $\eta_\kappa = 1$. This may be compared with the asymptotic result $a_c = 3.1$ and $R_c/\eta_\lambda\eta_v = 1745$ given by (4.16).

The case $P_m \ll 1$. In this case, magnetic diffusion is dominant and the additional term needed in expansions (4.1) is ($n = 0$, $k = 1$) and not ($n = 1$, $k = 0$). The corresponding governing equations at this order are

$$(\mathrm{D}^2 - a^2)(\mathrm{i}\omega_{00}\phi_{01} - \mathrm{D}h_{01}) = -R_{01}\theta_{00} - \mathrm{i}\omega_{01}(\mathrm{D}^2 - a^2)\phi_{00}, \tag{4.18a}$$

$$\mathrm{i}\omega_{00}h_{01} - \mathrm{D}\phi_{01} = -\mathrm{i}\omega_{01}h_{00} + (\mathrm{D}^2 - a^2)h_{00}, \tag{4.18b}$$

which are also subject to the boundary conditions (4.11). Further knowledge of the Hartmann layer is not required in solving the stability problem at this order. By carrying out an analysis similar to that of the previous subsection, we obtain

$$R_{01} = \frac{\Omega}{\eta_\kappa a^2}\left(\frac{\Omega_+\left[\omega_{00}^2 + aT(aT+2)\right]}{\omega_{00}^2 + aT(aT-2) + 4\Omega_+\eta_\kappa^2\Omega G_r}\right), \tag{4.19}$$

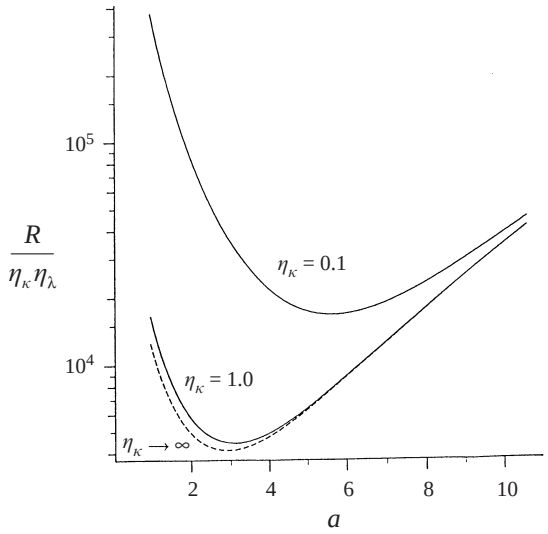

FIGURE 3. The neutral curves for thermal Alfvén waves in Case B when $P_m = 1$ for various values of η_κ. The critical Rayleigh number R_c is scaled. The asymptotic limit $\eta_\kappa \gg 1$ is represented by the dashed line.

while the expression for ω_{01} is the same as that for ω_{10} except that R_{10} is replaced by R_{01}. The asymptotic result replacing (4.16) is

$$R_{01} \sim \frac{\Omega^3 \eta_\kappa \left[\omega_{00}^2 + aT(aT+2)\right]}{a^2 \left[\omega_{00}^2 + aT(aT-2)\right] + \omega_{00}^2(\Omega F_1 + 4aF_2)} \quad \text{for } \eta_\kappa \to \infty, \tag{4.20}$$

and again $\omega_{01} \to 0$ in the same limit.

Table 3 gives several typical examples calculated from (4.6) and (4.19). This table shows that $a_c = 3.0$ and $R_c/\eta_\lambda \eta_\nu = 2562$ for $\eta_\kappa = 1$. This may be compared with the asymptotic result $a_c = 2.8$ and $R_c/\eta_\lambda \eta_\nu = 2353$ given by (4.20).

The case $P_m = O(1)$. Now both viscous and magnetic diffusion are important, the $(n = 0, k = 1)$ and $(n = 1, k = 0)$ terms are both needed in expansion (4.1). The final result is simply given by

$$R = R_{10}\eta_\nu + R_{01}\eta_\lambda, \quad \omega = \omega_{00} + \omega_{10}\eta_\nu + \omega_{01}\eta_\lambda. \tag{4.21a,b}$$

Several typical examples for $P_m = 1$ are shown in figure 3 for different values of η_κ together with the asymptotic result $\eta_\kappa \gg 1$. At $\eta_\kappa = 0.1$, the most unstable convection mode is $a_c = 5.6$ with $R_c/\eta_\lambda \eta_\kappa = 1.67 \times 10^4$. When η_κ is increased to 1.0, a_c diminishes to $a_c = 3.1$ and $R_c/\eta_\lambda \eta_\kappa = 4.44 \times 10^3$; the asymptotic results for $\eta_\kappa \to \infty$ are $a_c = 3.0$ and $R_c/\eta_\lambda \eta_\kappa = 2.97 \times 10^3$. It is relevant to § 6.2 below to observe that the leading-order asymptotic result for $\eta_\kappa \to \infty$, shown by the dashed line in figure 3, captures all the main features of the instability for moderate values of η_κ.

In summary, when the walls of the fluid layer are solid, perfect conductors, the Hartmann boundary layers on the walls play no role in determining a_c and R_c to leading order. The magnetoconvective motions are thermal Alfvén waves for any assigned values of P_m and η_κ, provided only that η_ν and η_λ are sufficiently small.

5. Case C: the exterior of the layer is a vacuum

5.1. *Undamped Alfvén waves*

This case for stress-free, perfectly insulating walls is somewhat different from Case B. The discontinuities in $\mathrm{D}\phi$ and $\mathrm{D}h$ across the Hartmann layers now play a role in determining R. The structure of the layers determines in a unique way how the discontinuities are related. When the exterior of the fluid layer is free space or is a light, perfectly insulating fluid, the zero stress conditions introduce Hartmann layers that require

$$\langle \mathrm{D}h \rangle = -\eta_v \langle \mathrm{D}^2\phi \rangle, \quad \text{at } z = \pm\tfrac{1}{2}; \tag{5.1a}$$

see, for example, Morley & Roberts (1997). In (5.1*a*), $\langle Q \rangle$ denotes the jump in a quantity Q from one side of the layer to the other. The physical content of (5.1*a*) is that, since the Hartmann layer is infinitely thin and has no mass, the net (viscous plus magnetic) stress acting across its edges must vanish. It is significant that the Hartmann layer thickness is of order $(\eta_v\eta_\lambda)^{1/2}$ so that within the boundary layer the D^2 terms in (4.2) are of order $1/\eta_v\eta_\lambda$, i.e. large compared with both the associated a^2 terms (except for wavenumbers too large, $a \geqslant O(\eta_v\eta_\lambda)^{-1/2}$, to be of interest here) and the $\mathrm{i}\omega/\eta_v$ and $\mathrm{i}\omega/\eta_\lambda$ terms, since $\omega = O(1)$. These terms can therefore be neglected to leading order. This means that the Hartmann layer jump condition is, to leading order, the local and t-independent (5.1*a*), even though the solution is unsteady. According to (5.1*a*), conditions (2.9*c*) and (2.9*d*) place a single demand on the mainstream:

$$\mathrm{D}h \pm ah + \mathrm{D}^2\phi = 0 \quad \text{at } z = \pm\tfrac{1}{2}. \tag{5.1b}$$

The leading-order equations ($n = k = 0$) are again (4.2*a–c*), but their solutions are subject to different boundary conditions, which by (2.9*a*), (2.9*b*) and (5.1*b*) are

$$\phi_{00} = \theta_{00} = \mathrm{D}h_{00} \pm ah_{00} = 0 \quad \text{at } z = \pm\tfrac{1}{2}. \tag{5.2a–c}$$

Again $R_{00} = 0$, and ϕ_{00} and h_{00} are given by (4.5) and (4.8), which automatically obey (5.2*a*). The dispersion relations obtained from (4.5*b*), (4.8*b*) and (5.2*c*) have real roots. The frequencies of the undamped Alfvén waves are solutions of

$$\omega_{00}(\omega_{00} + a\tan\tfrac{1}{2}\omega_{00}) + a^2(1 + \tanh\tfrac{1}{2}a) = 0, \tag{5.3a}$$

for the even modes, and

$$\omega_{00}(\omega_{00} - a\cot\tfrac{1}{2}\omega_{00}) + a^2(1 + \coth\tfrac{1}{2}a) = 0, \tag{5.3b}$$

for the odd modes. (The solutions $\omega_{00} = \pm\mathrm{i}a$ are spurious.) The most interesting solution is again the smallest root of (5.3*a*); it is displayed in figure 2, where it is seen to be quite different from the ω_{00} obtained in Case B. In this case

$$\omega_{00} \to \pi \quad \text{as } a \to 0 \quad \text{and as } a \to \infty, \tag{5.4a, b}$$

facts that will be useful below. It is found below that the marginal state always corresponds to the smallest ω_{00}. We shall later focus on this and also ignore modes from the odd-ϕ family.

5.2. *Thermal Alfvén waves*

The case $P_m \gg 1$. We shall keep this section brief as the analysis is similar to that of Case B. The stability problem for $P_m \gg 1$ again involves the term ($k = 0$, $n = 1$) in expansion (4.1). While the governing equations and the boundary condition (4.11*a*) for ϕ_{10} are exactly the same as in Case B, the boundary condition (5.1*b*) on h_{10} is

η_κ	a_c	R_c/P_r	ω_{00}
0.01	10.2	14.6	3.46
0.10	4.2	35.7	3.77
1.00	2.3	7.50×10^2	3.84
5.00	2.2	1.76×10^4	3.83

TABLE 4. Typical examples for Case C, $P_m \gg 1$.

quite different from (4.11*b*). We have

$$\phi_{10} = \mathrm{D}h_{10} + ah_{10} + \mathrm{D}^2\phi_{00} = 0 \quad \text{at } z = \tfrac{1}{2}. \tag{5.5a, b}$$

The real and imaginary parts of the solvability condition give rise to the Rayleigh number and a small correction to the frequency of the undamped Alfvén wave at the onset of convection:

$$R_{10} = \frac{\Omega\Omega_+\eta_\kappa^{-1}\left[\omega_{00}^2(2+a+aW^2) - 2a^2(1+T) - 4\omega_{00}^2\right]}{a^2\left[\omega_{00}^2(2+a+aW^2) - 2a^2(1+T)\right] + 4a^2\Omega\eta_\kappa^2(a\Omega_+G_r + 2\omega_{00}^2\Omega\Omega_+^{-1})}, \tag{5.6a}$$

$$\omega_{10} = -\frac{2a^2\omega_{00}R_{10}}{(2+a)\omega_{00}^2 - 2a^2 + a\omega_{00}^2W^2 - a^2T}\left\{\frac{4+a+T(2-aT)}{4\Omega} + \frac{\omega_{00}^2(2+a+aW^2) - 2a^2(1+T)}{4\Omega\Omega_+} - \frac{\eta_\kappa^3\Omega}{\omega_{00}}\left[\frac{\omega_{00}\Omega_-}{\eta_\kappa\Omega_+^2} + aG_i\right]\right\}, \tag{5.6b}$$

where $W = \tan\frac{1}{2}\omega_{00}$.

The physically realizable solution corresponds to the minimum Rayleigh number $R_c = (P_rR_{10})_{\min}$, which is obtained numerically. Our calculation, in which we use (5.3*a*) to find ω_{00} for a given a and then use (5.6*a*) to obtain R_{10}, indicates that there always exists a critical convection mode for any given non-zero η_κ. Several typical examples are given in table 4. The asymptotic expression for R_{10} as $\eta_\kappa \to \infty$ is

$$R_{10} \sim \frac{\eta_\kappa\Omega^3\left[\omega_{00}^2(2+a+aW^2) - 2a^2(1+T) - 4\omega_{00}^2\right]}{a^2\left[\omega_{00}^2(2+a+aW^2) - 2a^2(1+T)\right] + \omega_{00}^2\left[a\Omega F_1 + 4a^2(F_2+2)\right]}, \tag{5.7}$$

and $\omega_{10} \to 0$ in the same limit. The minimization of R_{10} over a in (5.6) gives rise to the critical mode $a_c = 2.2$, $R_c/\eta_\kappa\eta_v = 703$, which again is similar to the values of a_c and R_c for $\eta_\kappa = 1$ shown in table 4. The critical wavenumber is much smaller than in Case B.

The case $P_m \ll 1$. We now need the term ($n = 0$, $k = 1$) in expansions (4.1). The governing equations and the boundary condition for ϕ_{01} are the same as in Case B. But the boundary conditions replacing (5.5) are

$$\phi_{01} = 0, \quad \mathrm{D}h_{01} + ah_{01} = 0 \quad \text{at } z = \tfrac{1}{2}. \tag{5.8a, b}$$

Similar analysis as before leads to

$$R_{01} = \frac{\Omega\Omega_+\eta_\kappa^{-1}\left[\omega_{00}^2(2+a+aW^2) + 2a^2(1+T)\right]}{a^2\left[\omega_{00}^2(2+a+aW^2) - 2a^2(1+T)\right] + 4a^2\Omega\eta_\kappa^2(a\Omega_+G_r + 2\omega_{00}^2\Omega\Omega_+^{-1})}, \tag{5.9}$$

while the expression for ω_{01} is the same as (5.6*b*) with R_{01} replaced by R_{10}. The

η_κ	a_c	R_c/P_r	ω_{00}
0.01	11.0	17.47	3.44
0.10	4.3	48.84	3.76
1.00	2.2	1.050×10^3	3.83
5.00	2.2	2.466×10^4	3.83

TABLE 5. Typical examples for Case C, $P_m \ll 1$.

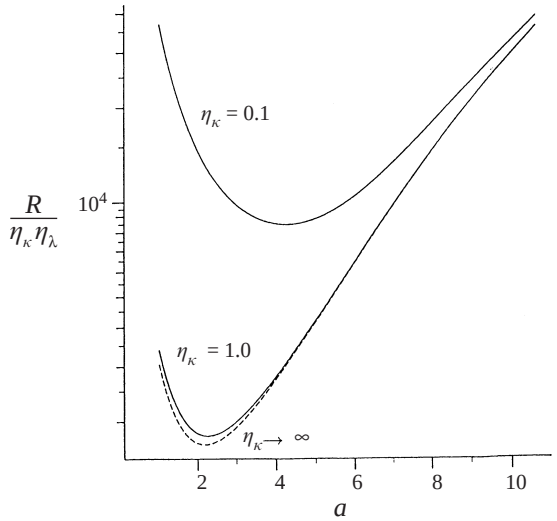

FIGURE 4. The neutral curves for thermal Alfvén waves in Case C when $P_m = 1$ for various values of η_κ. The critical Rayleigh number R_c is scaled. The asymptotic limit $\eta_\kappa \gg 1$ is represented by the dashed line.

asymptotic expression of R_{01} for $\eta_\kappa \to \infty$ is

$$R_{01} \sim \frac{\eta_\kappa \Omega^3 \left[\omega_{00}^2(2 + a + aW^2) + 2a^2(1 + T)\right]}{a^2 \left[\omega_{00}^2(2 + a + aW^2) - 2a^2(1 + T)\right] + \omega_{00}^2 \left[a\Omega F_1 + 4a^2(F_2 + 2)\right]}, \tag{5.10}$$

and $\omega_{01} \to 0$ in the same limit. Our calculations with (5.9) again suggests that there always exists a most unstable mode for any given η_κ. Some typical examples are given in table 5. When $\eta_\kappa \to \infty$, the asymptotic expression (5.10) gives $a_c = 2.2$ and $R_c/\eta_\lambda \eta_\kappa = 984$, which may be compared with the η_κ value in the table.

The case $P_m = O(1)$. Here both the terms $(n = 0,\ k = 1)$ and $(n = 1,\ k = 0)$ are required. The marginal state is simply described by

$$R = R_{10}\eta_\nu + R_{01}\eta_\lambda, \quad \omega = \omega_{00} + \omega_{10}\eta_\nu + \omega_{01}\eta_\lambda. \tag{5.11a,b}$$

A number of examples are shown in figure 4 for different values of η_κ together with the asymptotic result for $\eta_\kappa \to \infty$ for $P_m = 1$. For $\eta_\kappa = 0.1$, the most unstable mode is $a_c = 4.3$ with $R_c/\eta_\lambda \eta_\kappa = 8.46 \times 10^3$. When η_κ is increased to 1.0, the critical wavenumber a_c diminishes to $a_c = 2.3$ and $R_c/\eta_\lambda \eta_\kappa = 1.80 \times 10^3$. For asymptotically large η_κ, we obtain $R_c/\eta_\lambda \eta_\kappa = 1.56 \times 10^3$ and $a_c = 1.8$.

In summary, when the more realistic boundary conditions – stress-free, perfectly insulating walls – apply, the Hartmann layers play a role in determining a_c and R_c at leading order. Nevertheless, to leading order the magnetoconvective motions are

again thermal Alfvén waves for any assigned values of P_m and η_κ, provided only that η_ν and η_λ are sufficiently small.

6. Case D: solid insulating walls

6.1. *Undamped Alfvén waves*

Case D is quite different from both Cases B and C due to the greater significance of dissipation in the mainstream. Nevertheless, the role of the Hartmann layers is central and should be clarified at the outset.

The Hartmann jump condition is

$$\langle \mathrm{D}h \rangle = \mp P_m^{1/2} \langle \mathrm{D}\phi \rangle \quad \text{at } z = \pm\tfrac{1}{2}. \tag{6.1a}$$

According to (6.1*a*), conditions (2.10*c*) and (2.10*d*) place a single demand on the mainstream:

$$\mathrm{D}h \pm ah \pm P_m^{1/2} \mathrm{D}\phi = 0 \quad \text{at } z = \pm\tfrac{1}{2}, \tag{6.1b}$$

from which it follows that

$$\text{if} \quad P_m = \infty, \quad \mathrm{D}\phi = 0 \quad \text{at } z = \pm\tfrac{1}{2}, \tag{6.1c}$$

and

$$\text{if} \quad P_m = 0, \quad \mathrm{D}h \pm ah = 0 \quad \text{at } z = \pm\tfrac{1}{2}. \tag{6.1d}$$

A parallel exists here with the simpler situation of the attenuation of plane Alfvén waves (i.e. $a = 0$ waves) trapped between two boundaries (Hide & Roberts 1962; Roberts 1972). Here (6.1*c*) corresponds to perfectly conducting boundaries and (6.1*d*) to insulating boundaries. As Hide & Roberts remarked, when viscous and ohmic losses in the fluid are ignored, as we do to leading order, the waves are not damped in either of these extremes; they are attenuated by the boundaries only in intermediate cases where $P_m = O(1)$. In a similar way here, when $P_m = O(1)$, the Hartmann layers remove energy from the Alfvén waves even at leading order. The waves can be maintained only if buoyancy makes good the energy loss also at that order, and this requires that $R_{00} = O(1)$. It is not difficult to solve such $P_m = O(1)$ cases numerically. At leading order, the mainstream obeys (4.2) as before, and these equations must be solved subject to conditions (2.10*a*), (2.10*b*) and the Hartmann jump condition (6.1*b*). The condition that $\mathrm{Im}(\omega_{00}) = 0$ then determines R_{00} and the wave frequency $\mathrm{Re}(\omega_{00})$. We shall not carry out such a program here, mainly because it is not thematic to the objectives we set ourselves in § 1. Our aim is to consider situations in which the waves are non-dissipative at leading order, and in which R is determined at the next order. This can be done in the two limiting cases analogous to (6.1*c*) and (6.1*d*), $P_m \gg 1$ and $P_m \ll 1$, in which viscous losses and ohmic losses respectively dominate. Analytical expressions similar to those derived in Cases B and C are found. When $P_m \gg 1$, the leading-order solution, which describes undamped Alfvén waves, is exactly the same as in Case B; when $P_m \ll 1$, the leading-order solution is identical to that of Case C. The relevant ω_{00} are shown in figure 2.

We now turn to the role of dissipation in the mainstream. At first sight one is tempted to say that this must be negligible compared with the dissipation rate per unit area integrated through the Hartmann layers, because in dimensionless units they are respectively η_λ/ℓ and η_λ/δ_H ohmically and η_ν/ℓ and η_ν/δ_H viscously. If ℓ, the scale of convection in the mainstream, is $O(1)$ then it is indeed true that the dissipation in the Hartmann layer is all important. It transpires, however, that when

one retains that dissipation alone, the critical wavenumber for convection is infinite; see below. In fact, $\ell \ll 1$ for the critical mode, and dissipation in the mainstream is as important as it is in the Hartmann layers, and both must be retained if a_c and R_c is to be determined. In the following, we first establish that $a_c = \infty$ if mainstream dissipation is ignored, and we then modify the calculation of R by including that dissipation, again as a perturbation of the leading-order dissipationless waves. As usual, this procedure is valid only if $\eta_\nu \ll 1$ and $\eta_\lambda \ll 1$.

The results of our analysis of Cases B and C indicate clearly that the asymptotic limit for $\eta_\kappa \to \infty$ captures the main features of the instability even for η_κ as small as 1; this is also evident from figures 3 and 4. To simplify our analysis for Case D, we concentrate on the large-η_κ limit, in which the ω_{00} term in (4.2c) may be neglected to leading order.

6.2. *Thermal Alfvén waves: $P_m \gg 1$*

It has been emphasized in this paper that, to make a thermal Alfvén wave the most unstable mode of magnetoconvection, η_ν and η_λ must be small. Because $P_m \equiv \eta_\nu/\eta_\lambda \gg 1$ here, we may choose η_ν and $P_m^{-1/2}$ as the two small parameters for a double expansion of the solutions, replacing (4.1) by

$$R = \sum_{n=0}\sum_{k=0} P_m^{-n/2}\eta_\nu^k\, R_{nk}, \quad \omega = \sum_{n=0}\sum_{k=0} P_m^{-n/2}\eta_\nu^k\, \omega_{nk}, \quad \phi = \sum_{n=0}\sum_{k=0} P_m^{-n/2}\eta_\nu^k\, \phi_{nk}. \tag{6.2a–c}$$

On substituting (6.2) into (1.13)–(1.15) and expanding the relevant boundary condition in a similar way, we find that the leading-order ($k = 0$, $n = 0$) problem is the same as in Case B; see figure 2 for the most significant ω_{00}.

The governing equations for the ($n = 1$, $k = 0$) problem are

$$(\mathrm{D}^2 - a^2)\,(\mathrm{i}\omega_{00}\phi_{10} - \mathrm{D}h_{10}) = -R_{10}\theta_{00} - \mathrm{i}\omega_{10}(\mathrm{D}^2 - a^2)\phi_{00}, \tag{6.3a}$$

$$\mathrm{i}\omega_{00}h_{10} - \mathrm{D}\phi_{10} = -\mathrm{i}\omega_{10}h_{00}, \tag{6.3b}$$

which are subject to the boundary conditions

$$\phi_{10} = 0, \quad \mathrm{D}\phi_{10} + \mathrm{D}h_{00} + ah_{00} = 0 \quad \text{at } z = \tfrac{1}{2}. \tag{6.4a, b}$$

It follows that (4.12) can be replaced by the much simpler expression

$$\theta_{00} = \frac{a^2}{\eta_\kappa \Omega}\left[\frac{\cos\omega_{00}z}{\cos\frac{1}{2}\omega_{00}} - \left(\frac{T\Omega}{4a} + 1\right)\frac{\cosh az}{\cosh\frac{1}{2}a} + \frac{\Omega}{2a}\frac{z\sinh az}{\cosh\frac{1}{2}a}\right]. \tag{6.5}$$

By carrying out the analysis for the ($n = 1$, $k = 0$) problem, we obtain $\omega_{10} = 0$ in a by now familiar way; see (4.17). We also find that

$$R_{10} = \frac{16\eta_\kappa a\Omega^3}{Q_0 + Q_1 T + Q_2 T^2 + Q_3 T^3}, \tag{6.6}$$

where

$$Q_0 = -a\omega_{00}^4 + 11a^3\omega_{00}^2,$$

$$Q_1 = (a^2 + 2)\omega_{00}^4 + a^2(a^2 + 18)\omega_{00}^2 - 8a^4,$$

$$Q_2 = a\omega_{00}^4 - 7a^3\omega_{00}^2 + 4a^5, \quad Q_3 = -a^2\omega_{00}^2\Omega.$$

The R_{10} given by (6.6) is a monotonically decreasing function of a; by (4.7), we

have $R_{10}/\eta_\kappa = O(a^{-2})$ as $a \to 0$ and

$$R_{10}/\eta_\kappa \to \pi^2 \quad \text{as } a \to \infty. \tag{6.7}$$

In consequence, the Rayleigh number R_{10} has no minimum for $a = O(1)$ for any η_κ. It is also plausible that the minimum lies in the range $a \gg O(1)$. To determine this, additional terms in the expansion (6.2) are necessary because, for a sufficiently large wavenumber a, the term $(n = 0,\ k = 1)$ in the expansion becomes important. More precisely, when $a = O(\delta^{-3/4}\eta_\lambda^{1/2})$, where $\delta = (\eta_v\eta_\lambda)^{1/2}$ is the thickness of the Hartmann layer, the next-order term $(n = 0,\ k = 1)$ becomes so significant that it must be included. (The Hartmann jump condition (6.1*a*) is valid as long as $a \ll O(\delta^{-1})$, and a_c satisfies this requirement.)

The governing equations for the $(n = 0,\ k = 1)$ problem are given by (4.18*a*, *b*), but the boundary conditions are different from those considered in § 4. We now have

$$\phi_{01} = \mathrm{D}\phi_{01} = 0 \quad \text{at } z = \tfrac{1}{2}. \tag{6.8}$$

Since $\eta_\lambda = P_m^{-1}\eta_v$, the η_λ term in equation (1.10) would become important only in the higher-order $(n = 2,\ k = 1)$ approximation and can therefore be ignored here. The Rayleigh number R at the onset of instability is found to be

$$R \equiv P_m^{-1/2}R_{10} + \eta_v R_{01} = \frac{4\eta_\kappa a\Omega^3\left[4P_m^{-1/2} + (\omega_{00}^2 + aT(aT-2))\eta_v\right]}{Q_0 + Q_1T + Q_2T^2 + Q_3T^3}. \tag{6.9}$$

There are two main sources of ohmic dissipation: one arises from the Hartmann layers (the $P_m^{-1/2}$ term) and the other is the result of viscous losses in the mainstream (the η_v term). Our numerical calculation with (4.5*a*) and (6.9) suggests that the critical convection mode is, for any non-zero η_v, a thermal Alfvén wave. When $\eta_v \geqslant O(P_m^{-1/2})$, we have $a_c = O(1)$. When the Hartmann layer dissipation is dominant (i.e. when $\eta_v/P_m^{-1/2} \ll 1$), the critical wavenumber is large, of order $\delta^{-1}\eta_\lambda^{2/3}$, where $\delta = (\eta_v\eta_\lambda)^{1/2}$ is the thickness of the Hartmann layer. In this case, R_c takes the limiting value (6.7), although the approach to the limit is slow, since R_c deviates from (6.7) not by the order of the small parameter $\eta_v/P_m^{-1/2}$ but by a term proportional to its $\frac{1}{3}$ power. We show typical examples in figure 5 for different values of $P_m^{1/2}\eta_v$, where the dashed line represents the asymptotic limit $P_m^{1/2}\eta_v \to \infty$. For $\eta_v = P_m^{-1/2}$, equation (6.9) gives $a_c = 3.1$ and $R_c/\eta_v\eta_\kappa = 1974$.

6.3. *Thermal Alfvén waves: $P_m \ll 1$*

In this case, η_λ and $P_m^{1/2}$ are the natural small parameter for the double expansions:

$$R = \sum_{n=0}\sum_{k=0} P_m^{n/2}\eta_\lambda^k\, R_{nk},\quad \omega = \sum_{n=0}\sum_{k=0} P_m^{n/2}\eta_\lambda^k\, \omega_{nk},\quad \phi = \sum_{n=0}\sum_{k=0} P_m^{n/2}\eta_\lambda^k\, \phi_{nk}. \tag{6.10a–c}$$

The leading-order $(k = 0,\ n = 0)$ solution is exactly the same as in Case C, and the resulting ω_{00} is shown in figure 2. At the next order $(n = 1,\ k = 0)$ the solution is governed by equations (6.3), but the boundary conditions demand that

$$\phi_{10} = 0, \quad \mathrm{D}h_{10} + ah_{10} + \mathrm{D}\phi_{00} = 0 \quad \text{at } z = \tfrac{1}{2}. \tag{6.11a,b}$$

A similar analysis to that of § 6.2 again gives $\omega_{10} = 0$ and also

$$R_{10} = \frac{16\eta_\kappa\omega_{00}^2\Omega^3}{a(T_0 + T_1T + T_2T^2 + T_3T^3)}, \tag{6.12}$$

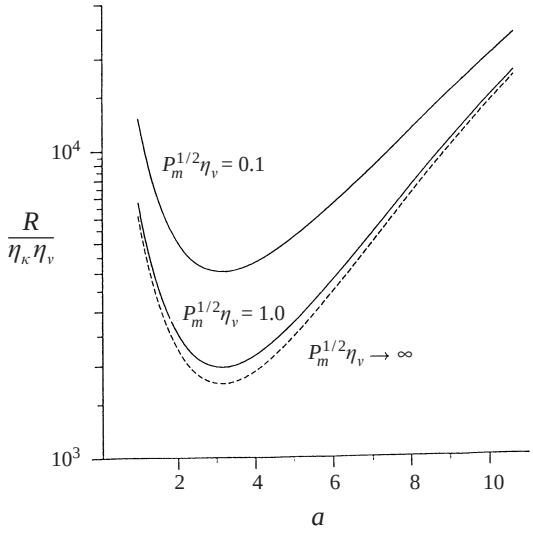

FIGURE 5. The neutral curves in Case D when $P_m \gg 1$ for various values of $P_m^{-1/2}\eta_v^{-1}$. The critical Rayleigh number R_c is scaled. The dashed curve applies when $P_m^{1/2}\eta_v \to \infty$.

where

$$T_0 = 3a\omega_{00}^4 + a^2(19a + 40)\omega_{00}^2 + 4a^4(a - 2),$$

$$T_1 = (a^2 + 2)\omega_{00}^4 + a^2(a^2 + 8a + 18)\omega_{00}^2 + 8a^4(a - 1),$$

$$T_2 = a\omega_{00}^4 - 7a^3\omega_{00}^2 + 4a^5, \quad T_3 = -a^2\omega_{00}^2\Omega.$$

Once more R_{10} is a monotonically decreasing function of a, and tends to the limiting value (6.7) as $a \to \infty$. The critical mode does not lie in the range $a = O(1)$ for any η_κ. This obstacle can again be overcome by including the $(n = 0, k = 1)$ terms in the expansions; these are significant when a is sufficiently large. They are governed by (4.10*a*, *b*), but are subject to different boundary conditions, namely

$$\phi_{01} = \mathrm{D}h_{01} + ah_{01} = 0 \quad \text{at } z = \tfrac{1}{2}. \tag{6.13}$$

It is found that $\omega_{10} = 0$ and that the Rayleigh number at the onset of magnetoconvection is given by

$$R \equiv P_m^{1/2}R_{10} + \eta_\lambda R_{01}$$
$$= \frac{4\eta_\kappa\Omega^3\left(4\omega_{00}^3P_m^{1/2} + [a\omega_{00}^2(4 + a) + \Omega(\Omega - 2a) + 2a^2(\Omega - a)T + a^4T^2]\eta_\lambda\right)}{a\omega_{00}(T_0 + T_1T + T_2T^2 + T_3T^3)}. \tag{6.14}$$

As before there are two main sources of dissipation: those associated with the Hartmann layers ($P_m^{-1/2}$ term) and the ohmic losses in the interior (the η_λ term). Our calculations based on (5.3*a*) and (6.14) indicate that a critical convection mode exists for all non-zero η_λ. When $\eta_\lambda \geqslant O(P_m^{1/2})$, it is found that $a_c = O(1)$. When the Hartmann layer dissipation dominates ($\eta_\lambda \ll O(P_m^{1/2})$), the critical wavenumber is large: $a_c = O(\delta^{-3/5}\eta_v^{-2/5})$. The approach to the limit (6.7) is even slower than in § 6.2; R_c deviates from (6.7) not by the order of the small parameter $P_m^{1/2}/\eta_\lambda$ but by a term

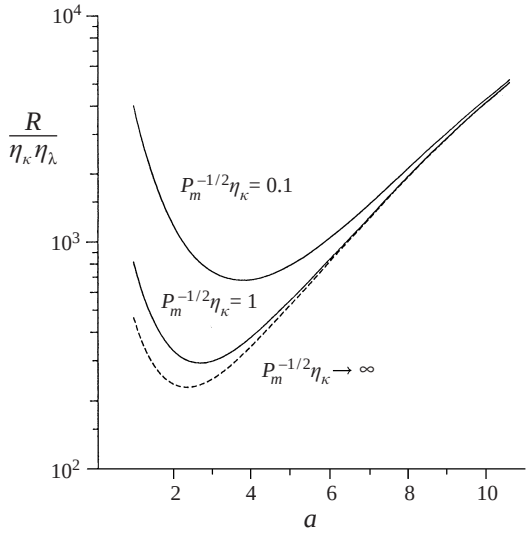

FIGURE 6. The neutral curves in Case D when $P_m \ll 1$ for various values of $P_m^{1/2}\eta_\lambda^{-1}$. The critical Rayleigh number R_c is scaled. The dashed curve applies when $P_m^{1/2}\eta_\lambda^{-1} \to 0$.

proportional to its $\frac{1}{5}$-power. Several examples are shown in figure 6, where the dashed line is for the asymptotic limit $P_m^{1/2}/\eta_\lambda \to 0$. When $\eta_\lambda = P_m^{1/2}$, equation (6.14) gives $a_c = 2.7$ with $R_c/\eta_\lambda\eta_\kappa = 291$.

7. Concluding remarks

In this paper, we have clarified several significant issues in one of the classical problems of MHD: time-dependent convection in an electrically-conducting fluid layer in the presence of a vertical magnetic field (Chandrasekhar 1961). We have found that, provided η_ν and η_λ are sufficiently small, the solutions are, at leading order, *undamped* Alfvén waves that merely advect the isothermal surfaces without diffusion; we called these 'thermal Alfvén waves'. In the next approximation, these waves are lightly damped, and are sustained by weak thermal buoyancy. (In contrast, the thermally excited Alfvén waves studied by Musman (1967), Savage (1969) and Parker (1974) are strongly damped thermally, even at leading order.)

The theory we have developed has many points of similarity with that governing oscillatory convection in a rapidly rotating Bénard layer when the Prandtl number is small (e.g. Zhang & Roberts 1997). For example, when $P_r = O(1)$, the rotational constraint causes the horizontal scale of the preferred convection pattern to diminish with increasing rotation; the concomitant increase in viscous dissipation causes the critical Rayleigh number to grow. This does not, however, happen in the $P_r \to 0$ limit, in which the preferred mode is oscillatory with $a_c = O(1)$. Since the convection is predominantly an inertial wave that requires little buoyancy to preserve it from viscous dissipation, the critical Rayleigh number is comparatively small. In a similar way, when $P_r = O(1)$ and $P_m = O(1)$, the magnetic constraint causes the horizontal scale of the preferred magnetoconvection mode to diminish with increasing applied field, and the associated enhancement in the viscous and ohmic dissipation causes the critical Rayleigh number to grow. We have found that, apart from two special subcases of D, the preferred oscillatory convection that arises when η_ν and η_κ are small

		$P_m \gg 1$	
Case	a_c	ω_c	R_c/η_v
A	2.2	3.14	$658\eta_\kappa$
B	3.1	5.30	$1745\eta_\lambda$
C	2.2	3.83	$703\eta_\kappa$
D	∞	3.14	$9.87P_rP_m^{-1/2}$
		$P_m \ll 1$	
Case	a_c	ω_c	R_c/η_λ
A	2.2	3.14	$658\eta_\kappa$
B	2.8	5.43	$2353\eta_\lambda$
C	1.8	3.83	$1560\eta_\kappa$
D	∞	3.14	$9.87P_rP_m^{-1/2}$

TABLE 6. Summary comparing Cases A–D.

has a horizontal scale comparable with the depth of the layer ($a_c = O(1)$). Since the convection is predominantly an Alfvén wave that requires little buoyancy to preserve it from viscous and ohmic dissipation, the critical Rayleigh number is comparatively small. The two types of convection are however rather different mathematically. The inertial wave arising at leading order in the rotating layer is governed by a second-order equation. In contrast, the Alfvén wave excited here is not purely transverse and is therefore associated with a pressure disturbance; the governing equation is therefore of fourth order.

The principal theme of this paper is that boundary layers arise in all situations except that of the illustrative Case A. In Case C, of free boundaries, the Hartmann layers are weak and the results are qualitatively the same as in Case A, but not quantitatively of course, as is seen in the results in table 6. Cases B and D are, however, qualitatively completely different, and even depend on the diffusivities in a different way from Cases A and C. It is inappropriate to summarize all the conclusions of §§ 4 and 6 here and we merely focus in table 6 on the results for $\eta_\kappa \to \infty$ in Cases A–C, and for $\eta_v + \eta_\lambda \ll P_m^{-1/2}$ in Case D.

Since Chandrasekhar wrote his book, magnetoconvection has been extensively studied in various geometries and with both uniform and spatially varying applied magnetic fields; the subject has been reviewed by Proctor & Weiss (1982), Fearn, Roberts & Soward (1988), Hughes & Proctor (1988), Weiss (1991), Proctor (1992), Nordlund *et al.* (1993) and Cattaneo (1994). Further relevant references can be found in these surveys. We believe that the present paper represents the first study of convection in the form of pure Alfvén waves, by which we mean waves that at leading order are completely undamped; previous studies have linked convection to thermally damped Alfvén waves, which required buoyant energy input at leading order. An extension of the present study to the case where both rotation and magnetic field act is under way. Other models where curvature effects are significant will also be investigated in the future.

While at Exeter, P.H.R. was supported by the PPARC grant GR/K79493; while at UCLA he is supported by NSF grants EAR97-25627 and ATM-12546. K.Z. is partly supported by NATO Grant CRG 971513 and by a NERC grant. We thank these fund granting agencies for giving us the opportunity of working together.

REFERENCES

Blanchflower, S. M., Rucklidge, A. M. & Weiss, N. O. 1998 Modelling photospheric magneto-convection. *Mon. Not. R. Astron. Soc.* **301**, 593–608.

Cattaneo, F. 1994 Magnetoconvection. In *Solar Magnetic Fields* (ed. M. Schüssler & W. Schmidt), pp. 261–281. Cambridge University Press.

Chandrasekhar, S. 1952 On the inhibition of convection by a magnetic field. *Phil. Mag.* (7) **43**, 501–532.

Chandrasekhar, S. 1961 *Hydrodynamic and Hydromagnetic Stability*. Clarendon (referred to herein as C61).

Fearn, D. R., Roberts, P. H. & Soward, A. M. 1988 Convection, stability and the dynamo. In *Energy, Stability and Convection* (ed. B. Straughan & P. Galdi), pp. 60–324. Longman.

Gibson, R. D. 1966 Overstability in the magnetohydrodynamic Bénard problem at large Hartmann number. *Proc. Camb. Phil. Soc.* **62**, 287–299.

Gilman, P. A. & Miller, J. 1981 Dynamically consistent nonlinear dynamos driven by convection in a rotating spherical shell. *Astrophys. J. Suppl.* **46**, 211–238.

Glatzmaier, G. A. 1984 Numerical simulations of stellar convective dynamos. I. The model and the method. *J. Comput. Phys.* **55**, 461–484.

Hide, R. & Roberts, P. H. 1962 Some elementary problems in magneto-hydrodynamics. *Adv. Appl. Mech.* **4**, 215–316.

Howard, R. F. & Labonte, B. J. 1981 Surface magnetic fields during the solar activity cycle. *Solar Phys.* **74**, 131–145.

Hughes, D. W. & Proctor, M. R. E. 1988 Magnetic fields in the solar convection zone: magneto-convection and magnetic buoyancy. *Ann. Rev. Fluid Mech.* **20**, 187–223.

Hurlburt, N. E., Proctor, M. R. E., Weiss, N. O. & Brownjohn, D. P. 1989 Nonlinear compressible magnetoconvection. Part 1. Travelling waves and oscillations. *J. Fluid Mech.* **207**, 587–628.

Kagayama A., Sato, T., Watanabe, K., Horiuchi, R., Hayashi, T., Todo, Y., Watanabe, T. H. & Takamara, H. 1995 Computer simulation of a magnetohydrodynamic dynamo. *Phys. Plasmas* **2**, 1421–1431.

Morley, N. E. & Roberts, P. H. 1997 Solutions of uniform, open-channel, liquid metal flow in a strong, oblique magnetic field. *Phys. Fluids* **8**, 923–935.

Musman, S. 1967 Alfvén waves in sunspots. *Astrophys. J.* **149**, 201–209.

Nordlund, Å., Galsgaard, K. & Stein, R. F. 1993 Magnetoconvection and magnetoturbulence. In *Solar Surface Magnetism* (ed. R. J. Rutten & C. J. Schrijver), pp. 471–498. Kluwer.

Parker, E. N. 1974 The nature of the sunspot phenomenon. II. Internal overstable modes. *Solar Phys.* **37**, 127–144.

Proctor, M. R. E. 1992 Magnetoconvection. In *Sunspots: Theory and Observations* (ed. J. H. Thomas & N. O. Weiss), pp. 221–241. Kluwer.

Proctor, M. R. E. & Weiss, N. O. 1982 Magnetoconvection. *Rep. Prog. Phys.* **45**, 1317–1379.

Roberts, P. H. 1967 *An Introduction to Magnetohydrodynamics*. Elsevier.

Roberts, P. H. 1972 Electromagnetic core-mantle coupling. *J. Geomag. Geoelectr.* **24**, 231–259.

Savage, B. D. 1969 Thermal generation of hydromagnetic waves in sunspots. *Astrophys. J.* **156**, 707–728.

Steiner, O., Grossmann-Doerth, U., Knölker, M. & Schüssler, M. 1994 Simulation of magneto-convection with radiative transfer. In *Solar Magnetic Fields* (ed. M. Schüssler & W. Schmidt), pp. 286–287. Cambridge University Press.

Thompson W. B. 1951 Thermal convection in a magnetic field. *Phil. Mag.* (7) **42**, 1417–1432.

Wang, T.-M., Sheeley, N. P. & Nash, A. G. 1991 A new solar cycle model including meridional circulations. *Astrophys. J.* **383**, 431–442.

Weiss, N. O. 1991 Magnetoconvection. *Geophys. Astrophys. Fluid Dyn.* **62**, 229–247.

Zhang, K. & Roberts, P. H. 1997 Thermal inertial waves in a rotating fluid layer: exact and asymptotic solutions. *Phys. Fluids* **9**, 1980–1987.